IOPscience iopscience.iop.org

Home Search Collections Journals About Contact us My IOPscience

Unusual multilayer relaxation of the Mo(111) surface induced by hydrogen

This article has been downloaded from IOPscience. Please scroll down to see the full text article.

1999 J. Phys.: Condens. Matter 11 1873

(http://iopscience.iop.org/0953-8984/11/8/002)

View the table of contents for this issue, or go to the journal homepage for more

Download details:
IP Address: 171.66.16.214
The article was downloaded on 15/05/2010 at 07:06

Please note that terms and conditions apply.

J. Phys.: Condens. Matter **11** (1999) 1873–1888. Printed in the UK PII: S0953-8984(99)98885-9

Unusual multilayer relaxation of the Mo(111) surface induced by hydrogen

M Arnold†, A Fahmi‡, W Frie†, L Hammer† and K Heinz†

† Lehrstuhl für Festkörperphysik, Universität Erlangen–Nürnberg, Staudtstrasse 7, D-91 058 Erlangen, Germany

‡ Fritz-Haber-Institut der Max-Planck-Gesellschaft, Faradayweg 4–6, D-14 195 Berlin-Dahlem, Germany

Received 30 October 1998, in final form 18 November 1998

Abstract. The atomic structures of clean and hydrogen-saturated Mo(111) surfaces were investigated by quantitative structure analyses combining low-energy electron diffraction and density functional theory (DFT) calculations. Both methods corroborate, in good agreement, the pronounced contraction of the top two interlayer spacings for the clean surface predicted theoretically earlier. Upon hydrogen saturation with three adatoms per surface unit cell, the drastic contraction of the uppermost interlayer distance is not reduced as usually observed for other surfaces, but remains practically unchanged. In contrast, the second interlayer spacing de-relaxes completely to the bulk value. Hydrogen is found to adsorb at sites with twofold coordination, bonding to atoms of the top two substrate layers, shifted off the ideal bridge position.

1. Introduction

The adsorption of hydrogen on transition metal surfaces has been subject to a large number of investigations since the early days of surface science (for reviews see, e.g., references [1, 2]). More recently, much effort has been spent on also quantitatively deriving—in particular—the geometry of the adsorption structure, including both the adatoms' sites and the structural modification of the substrate induced by adsorption, in order to provide the basis for a detailed microscopic understanding. In the large majority of cases, the hydrogen atoms are found to adsorb at the most highly coordinated sites offered by the substrate, if this is allowed by the hydrogen–metal bond lengths and the reconstructive movements of substrate atoms. So, fourfold-coordinated hollow sites on fcc(100) surfaces, threefold-coordinated hollow sites on close-packed or nearly close-packed surfaces and on microfacets of fcc(110) surfaces, or twofold-coordinated bridge sites on bcc(100) surfaces have been obtained [3]. Also, as detected only very recently in the case of the c(2×2)–3H phases on the more open surfaces Re(10$\bar{1}$0) and Ru(10$\bar{1}$0) [4], the simultaneous occupation of bridge and hollow sites can take place. At the rather high coverage of 3/2 (equivalent to an average hydrogen density of 1.2×10^{15} atoms cm^{-2}), the occupation of differently coordinated sites was interpreted as being possibly due to the competition between the local energy gain by the H–metal bonding and adatom–adatom repulsion. The latter seems to 'win', because the energy difference between bridge and hollow sites amounts to only several tens of meV [4].

In the present paper we also investigate the adsorbate geometry of hydrogen on a rather open surface, i.e. that of Mo(111). The openness of the surface is equivalent to a considerable surface roughness, demonstrated by the perspective view displayed in figure 1.

0953-8984/99/081873+16$19.50 © 1999 IOP Publishing Ltd

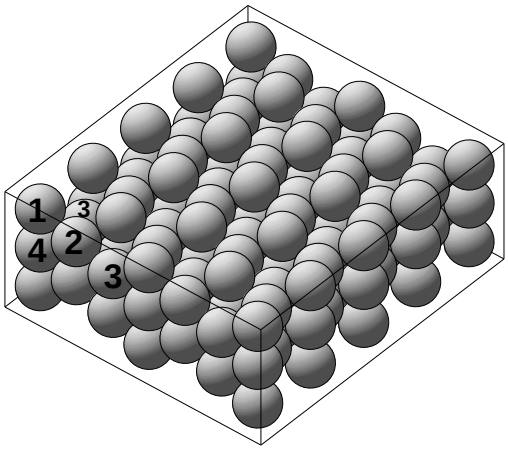

Figure 1. A perspective view of an elemental bcc(111) surface.

This surface openness/roughness leads to large and non-alternating relaxations of spacings $d_{i,i+1}$ between layers i and $i+1$ of bcc(111) metal surfaces, as predicted by total-energy calculations [5–7]. So, for Mo(111) the first six spacings have been calculated by tight-binding-type [5] and local density functional calculations using pseudopotentials [7] yielding for, e.g., the top two spacings $\Delta d_{12}/d_0 = -19.7\%$, $\Delta d_{23}/d_0 = -7.6\%$ and $\Delta d_{12}/d_0 = -18.7\%$, $\Delta d_{23}/d_0 = -20.3\%$, respectively, where $d_0 = 0.9072$ Å is the bulk interlayer distance. However, these theoretical results are not corroborated by experiments applying low-energy ion scattering (LEIS) [8] which, though in agreement with the strong contraction of the first spacing, yield a slight expansion of d_{23}. For Fe(111), structure determination by quantitative low-energy electron diffraction (LEED) is in agreement with the general prediction, finding $\Delta d_{12}/d_0 = -16.9\%$ and $\Delta d_{23}/d_0 = -9.8\%$ [9], but again (medium-energy) ion scattering (MEIS) yields an expansion of the second spacing [10]. For Mo(111), we aim to resolve this discrepancy as the first issue of the present paper.

The second and main aim of the paper, however, is that of deriving the adsorption structure of hydrogen on Mo(111) at full coverage, i.e. three adatoms per unit cell, for which in LEED a 1×1 diffraction pattern is observed. The analyses presented below include both the geometry of the adsorption site and the reaction of the substrate upon adsorption, i.e. in the case of a 1×1 phase the adsorption-induced modification of the multilayer relaxation. As, to the authors' knowledge, this is the first quantitative structure determination for a H/bcc(111) system, the present investigation—besides giving quantitative structural information for the special system Mo(111)-(1×1)–3H—might be representative as regards the general properties of H/bcc(111). In practically all hydrogen adsorption systems investigated quantitatively, hydrogen saturation was found to lead to a de-relaxation of the top interlayer spacing towards the bulk value [3]. This holds also for bcc metal surfaces as shown e.g. for both the (110) [11,12] and (100) [13,14] surfaces of molybdenum and tungsten. So, it is interesting to investigate whether the very open Mo(111) surface with its—as will be confirmed by the present analysis—non-oscillatory layer relaxation in the clean state will exhibit the same features upon hydrogen adsorption. Moreover, we aim to derive the adatom adsorption sites. We recall that, consistently with the general findings, bridge sites and threefold-coordinated sites have been detected on Mo(100) [15] and Mo(110) [11], respectively.

In a joint effort we apply in parallel density functional theory (DFT) and quantitative

LEED to derive the full structure of the surface, i.e. both the adsorption sites and the adsorbate-induced change of the substrate multilayer relaxation. As we can safely assume that hydrogen does not go below the surface due to the low solubility of hydrogen in molybdenum, and as there are no indications for the existence of several structural phases for the coverage under investigation, the combination of the two methods is rather ideal. On the one hand, it combines theoretically and experimentally based methods. On the other hand, dynamical LEED analysis is rather powerful and reliable for determining the multilayer relaxation of the strongly scattering substrate, where an accuracy in the percentage region is usually achieved. Although in principle the method is also sensitive to hydrogen and its position, as has been demonstrated by a number of quantitative structure determinations (for a catalogue and recent review, see reference [3] and reference [16], respectively), the weakness of the scattering by hydrogen makes the determination of the adatom site rather uncertain, leading to positional error limits of the order of ± 0.5 Å. In the present case, the situation is even worse due to the absence of superstructure spots and additionally to the presence of as many as three hydrogen atoms in the surface unit cell. Here, DFT plays the leading part, as it does not suffer from the low scattering strength of hydrogen. Moreover, in general it also reliably predicts the substrate's structural and electronic reaction to the adsorbate. Yet, if total energies calculated for different models, i.e. different adsorption sites combined with different substrate relaxations, turn out to be very close, only the reliable knowledge of the latter from the LEED analysis allows us to choose the correct model.

The paper is organized as follows. The next two sections describe experimental details and computational methods applied for the LEED and DFT calculations. In section 3 we concentrate on the analysis of the clean Mo(111) surface, whilst section 4 describes the interplay between LEED and DFT allowing one to reliably determine the structure of (1×1)–3H/Mo(111). In the last section the results are discussed.

2. Experimental and computational details of the analyses

2.1. Sample preparation and LEED measurements

The experiments were performed in an ultrahigh-vacuum chamber with a base pressure below 5×10^{-11} mbar. A four-grid back-view LEED optics was used both for intensity measurements and—operated in the retarding-field mode—Auger electron spectroscopy (AES). The sample could be heated up to 2500 K by electron bombardment from the rear and cooled to below 100 K by direct contact with a liquid-nitrogen reservoir. A $WRe_{3\%}$–$WRe_{25\%}$ thermocouple directly attached to the sample was used to measure the temperature. Linear and rotational degrees of freedom of the sample manipulator enabled precise adjustment of the crystal orientation to be carried out in order to ensure normal incidence of the primary electron beam.

After a few sputter/annealing cycles, the crystal was heated to about 1500 K in an oxygen ambient of 2×10^{-7} mbar for a total of ten hours to exhaust the bulk carbon impurities. The remaining oxygen was removed by a flash to 2400 K. Afterwards, a sharp (1×1) LEED pattern with very low background was observed with no traces of contamination detectable by AES. In the course of the measurements, repeated flashes to 2400 K were carried out to remove residual gas contamination of the surface. Hydrogen was already made to adsorb with a partial pressure of about 10^{-8} mbar during the cooling period to below 100 K. No superstructures were found for any hydrogen coverage up to saturation, even at low temperature. By analogy with the structurally closely related and substitutionally disordered alloy surface $Mo_{0.75}Re_{0.25}(111)$, for which a nuclear reaction analysis (NRA) found the maximum coverage of hydrogen to be three atoms per unit cell [17], we conclude that for elemental Mo(111) too, saturation corresponds to

this coverage. This is further supported by a study of thermodesorption of hydrogen from the structurally related W(111) surface exhibiting practically the same saturation coverage [18].

LEED intensity versus energy spectra, $I(E)$, were measured with the sample near liquid-nitrogen temperature and for normal incidence of the primary electron beam. A computer-controlled video technique was used, allowing for fast data acquisition (given by the video rate of 20 ms/half-frame) and for on-line background correction as described in detail elsewhere [19–21]. The normal incidence was adjusted by comparison of symmetrically equivalent beams. Averaging of intensities both from repeated measurements of a single beam (four times) and for beams symmetrically equivalent at normal incidence leads to a considerable improvement of the signal-to-noise ratio. The corresponding effective speed of measurement amounts to about 5 min for one set of symmetrically equivalent beams. After this period of time, the clean surface was flashed to 2000 K to remove possible contamination from residual gas which could affect the multilayer relaxation. In contrast, the hydrogen-saturated surface turned out to be much more inert against contamination, and thus a whole database could be collected from one single preparation. The primary beam current was measured in parallel and used for normalization of the spectra. Residual noise in the spectra was removed by final three-point smoothing. For the clean surface, the resulting database as input to the intensity analysis consists of the $I(E)$ spectra of 13 symmetrically inequivalent beams measured between 50 and 500 eV in steps of 0.5 eV. This amounts to a database of total energy width $\Delta E = 3590$ eV for the clean surface. For the hydrogen-saturated surface, the total energy width is similar, $\Delta E = 3630$ eV.

2.2. LEED intensity calculations

For the LEED intensity calculations, bcc(111) surfaces are special, due to their small interlayer spacings, which in the case of Mo(111) amount to $d_0 = 0.9072$ Å in the bulk and may be even smaller at the surface due to interlayer relaxations. This inhibits the application of fast standard methods for the stacking of layers, such as renormalized forward scattering (RFS) or layer doubling (LD) [22, 23], i.e. to calculate the surface scattering matrix from those of the layers using the plane-wave representation. The general way out of this difficulty is to use the angular momentum representation [9, 24, 25]. The most rigorous procedure is that of treating the whole surface as a composite layer made up by a finite number of Bravais-lattice layers and of calculating its diffraction in the angular momentum representation. Of course, this is a rather CPU-time-consuming process, as the computational effort necessary to invert the corresponding matrix scales with N^3, where N is the number of layers to be considered as determined by electron attenuation, which in turn is described by the imaginary part V_{0i} of the inner potential. In the present case of Mo(111), corresponding to $V_{0i} = -5.5$ eV, a total of $N = 18$ layers proved to be sufficient for energies up to 500 eV. Although this can readily be handled by today's workstations, the necessary CPU time 'explodes' when the intensities of a high number of test models must be calculated in order to derive the best-fit structure. Therefore, the perturbation method TensorLEED [26–28] was applied, which allows one to circumvent the full recalculation of the surface diffraction for each test structure. Additionally, we used an automated search procedure [29] to locate the best-fit structure in the multi-dimensional parameter space. Up to 11 phase shifts were used (calculated relativistically and spin averaged for Mo); these had been applied successfully for the analysis of H/Mo(110) [11, 30]. They were corrected for isotropic thermal vibrations in the usual way [22], where for layers below the second Mo layer a Debye temperature of 450 K [31] was used. For the first two Mo layers and the H layer, the vibrational amplitudes were fitted to the experimental data in the course of the analysis, where the amplitudes of the hydrogen and the

top Mo atoms were assumed to be the same as those also successfully applied earlier [30, 32]. For the quantitative comparison of experimental and calculated spectra, the Pendry R-factor was used [33].

The application of TensorLEED for the determination of the multilayer relaxation requires some caution. It is obvious that the change of a deep-lying interlayer spacing simultaneously changes the position of all layers above. So, the perturbation of the surface structure with respect to the reference structure can be rather large and may be outside the validity range of TensorLEED. Therefore, repeated reference structure calculations should be performed until convergence is achieved. In the present case, starting with bulk-like layer spacings as the initial reference, two additional reference calculations were carried out, whereby the deviations of the eventual best-fit structure were less than 0.05 Å from the last reference for all spacings. Because of the small value of the bulk spacing, we allowed for the variation of as many as ten interlayer distances within the structural search. After convergence of the structural search, the vibrational amplitudes and the imaginary part of the inner potential were fine tuned. Finally, leaving the best-fit geometry fixed, the energy dependence of the real part of the inner potential was adjusted, which, however, turned out to be rather weak, i.e. -10.0 eV + $0.006E$ for the clean surface and -10.1 eV + $0.003E$ for the hydrogen-covered surface.

For the estimation of errors, usually the variance of the R-factor is applied:

$$\mathrm{var}(R) = R\sqrt{8V_{0i}/\Delta E}$$

where R is the minimum R-factor achieved [33]. Neglecting correlations between parameters, the error limit for a certain parameter is determined by the corresponding R-factor reaching the value $R + \mathrm{var}(R)$. Again, for the reasons given above, this means that the error limits resulting in this way for deep-lying layers are substantially underestimated. Only for the top-layer spacing can the determination of the errors be considered reliable. This is the case in the analyses below, and provides an idea of the corresponding values for deeper spacings if one considers that the sensitivity of LEED decreases with increasing depth because of electron attenuation.

2.3. DFT calculations

As already mentioned, density functional theory was applied to determine surface relaxations, adsorption sites of hydrogen and hydrogen-induced surface relaxation. The calculations were made for zero temperature with zero-point vibrations neglected. The exchange–correlation was treated by the generalized gradient approximation (GGA) [34], and for the self-consistent solution of the Kohn–Sham equations a full-potential linearized augmented-plane-wave (FP-LAPW) method was used [35, 36]. Geometry optimizations were realized within a damped molecular dynamics approach [37]. The molybdenum valence 4d5s5p and semicore 4s4p (core) electrons were treated scalar (fully) relativistically and the muffin-tin (MT) radii for hydrogen and molybdenum were chosen as 0.48 Å and 1.22 Å, respectively (note that the interatomic distance in molybdenum bulk is 2.72 Å). For the basis sets, radial functions inside MT spheres up to $l_{\max} = 12$ and a plane-wave-basis expansion in the interstitial region up to $K_{\mathrm{wf}}^2 = 217.6$ eV were used. For the potential, the (l, m) representation within each MT sphere was taken up to $l_{\max} = 6$, whereas the kinetic energy cut-off for the interstitial region was set to $G_{\mathrm{pot}}^2 = 1958.4$ eV. Fermi smearing with a broadening of $kT_{\mathrm{el}} = 0.068$ eV was used to stabilize the self-consistency and k-summation. Calculations for Mo bulk with a set of 120 special k-points, which correspond to a Monkhorst–Pack division of 15–15–15, give lattice parameters of 3.13 Å (LDA), 3.16 Å (GGA) and 3.17 Å (GGA + scalar relativistic correction for valence electrons) to be compared with the experimental value of 3.14 Å. For the slab

calculations, we use a set of seven special k-points, which correspond to a Monkhorst–Pack division of 6–6–1.

The Mo(111)-(1 × 1) surface was modelled by five-, seven- and nine-layer slabs repeated in the z-direction and separated by a vacuum region whose thickness is larger than 9.5 Å. This value was optimized such that interactions between successive slabs (in the z-direction) are negligible. For the H/Mo system, first a hypothetical (1 × 1)–1H phase was calculated in order to determine the most favourable adsorption site for a single hydrogen atom in the unit cell. Subsequently, the experimentally observed (1 × 1)–3H phase was treated. Hydrogen atoms were positioned on both sides of the slab to avoid extra interactions due to adsorbate-induced surface dipoles. The central layer, which contains the symmetry centre of the slab, was fixed during geometry optimizations. Five- and seven-layer models for both clean and hydrogen-covered surfaces produced considerable relaxations even for the deepest spacing in the slab, indicating too thin a slab. Only the nine-layer slab yielded—as is necessary for convergence—the bulk-like value for the deepest spacing and, consistently, only then was agreement with the LEED results achieved. Therefore, the minimum model for a bcc(111) surface should contain nine layers, in rough agreement with the treatment of the more compact fcc(111) surfaces for which, due to the larger layer spacings, five-layer models prove to be sufficient [38–40]. Discussions of the results will focus on the nine-layer slab.

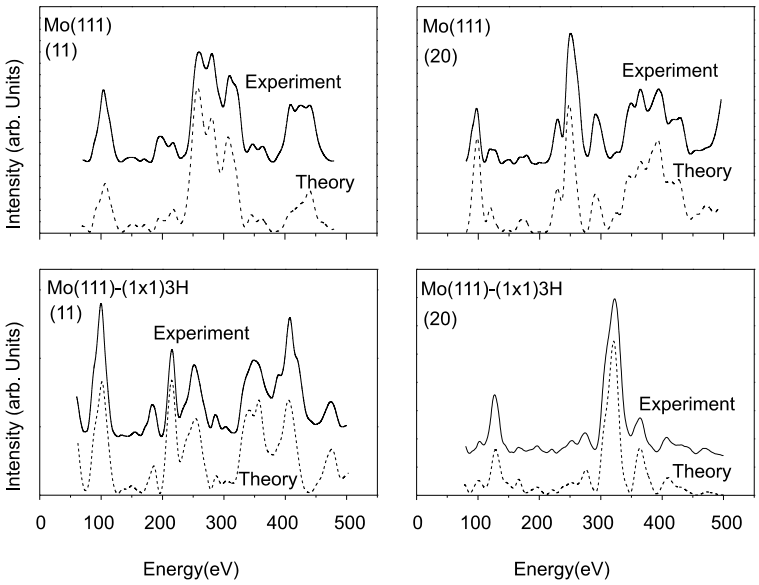

Figure 2. Comparison of experimental and calculated best-fit $I(E)$ spectra for two selected beams of the clean (top) and hydrogen-saturated (bottom) surface of Mo(111).

3. Analyses of the clean surface

3.1. Results from LEED

The best-fit structure determined by LEED intensity analysis for the clean surface clearly corroborates the earlier theoretical prediction of a considerable contraction of the first two interlayer spacings. It turns out that they are contracted by almost the same amount

Table 1. Multilayer relaxation of the clean Mo(111) surface as determined by DFT for five-, seven- and nine-layer slabs and by LEED. The bulk interlayer spacing amounts to $d_0 = 0.9072$ Å.

	DFT			
	5L	7L	9L	LEED
$\Delta d_{12}/d_0$ (%)	−8	−13	−23	−18.8
$\Delta d_{23}/d_0$ (%)	−23	−17	−21	−18.9
$\Delta d_{34}/d_0$ (%)	—	+ 6	+ 12	+ 6.4
$\Delta d_{45}/d_0$ (%)	—	—	+ 1	+ 2.2
$\Delta d_{56}/d_0$ (%)	—	—	—	+ 2.1
$\Delta d_{67}/d_0$ (%)	—	—	—	+ 0.9

($\Delta d_{12}/d_0 = -18.8\%$, $\Delta d_{23}/d_0 = -18.9\%$). As displayed in the right-hand column of table 1, the next spacing d_{34} is moderately expanded, whilst all deeper spacings deviate only by about 2% or less from the bulk value, and the question arises of whether or not these deviations are significant. As argued above, the slab calculation by TensorLEED prohibits a reliable determination of error limits for the values of $d_{i,i+1}$ for $i \geqslant 2$. An estimate is obtained by the calculation of the error limit for d_{12}, which yields $\pm 1.6\%$ for a minimum Pendry R-factor of $R = 0.15$ and a variance $\mathrm{var}(R) = 0.017$. As the accuracy of LEED tends to decrease with increasing depth due to electron attenuation, we expect the error limits for deeper spacings to be larger than 2%, i.e. the values for $d_{i,i+1}$ for $i \geqslant 3$ are bulk-like within the limits of errors. Therefore, we do not display values for deeper spacings ($i \geqslant 6$) in table 1. We emphasize, however, that the reproduction of the bulk value within the expected limits of errors demonstrates the stability and reliability of the structural search procedure applied. The low minimum R-factor corresponds to a very satisfactory agreement between experimental and calculated best-fit spectra, as is also evident from visual inspection of the spectra in the top panels of figure 2.

3.2. Results from DFT

In order to calculate the surface multilayer relaxation, the positions of the different layers of a slab are allowed to move vertically (with the exception of the centre layer which is fixed) until the energy minimum is found. Table 1 displays the results for slabs made up of five, seven and nine layers. From the layer spacings derived, it becomes immediately clear that only the result for the nine-layer slab can be reliable, because only for this case is the spacing between the centre layer and its neighbour practically bulk-like, i.e. this slab is regarded as modelling the semi-infinite surface sufficiently closely. Its energy is lowered by 0.79 eV per unit cell and surface relative to that of the unrelaxed slab obviously, due to an increased bonding between surface atoms, as will be discussed later. Not surprisingly, it is the nine-layer-slab calculation for which DFT and LEED agree best. At the percentage level, the agreement seems to be limited, as the results can differ by of the order of 5%. However, we emphasize that due to the small layer spacings this translates to absolute differences of less than 0.05 Å. One should also recall that the DFT calculations refer to zero temperature whilst the LEED data were taken at about 90 K. Moreover, the general features determined by the two methods are very much the same: the first two spacings are drastically and almost equally contracted (by of the order of 20%) whilst the third spacing is expanded by a considerably smaller amount. Deeper spacings are practically bulk-like.

4. DFT test calculations for an assumed Mo(111)-(1 × 1)–1H structure

As the situation becomes rather complex with as many as three atoms adsorbed in the unit cell, we concentrate first on a single hydrogen atom within the unit cell in order to get a feeling for its influence. Upon adsorption of hydrogen atoms and their bonding with molybdenum atoms, the Mo–Mo bonds within the surface should weaken and a de-relaxation of the surface is expected to result. In a first-order approximation the total energy, i.e. the adsorption energy W, can be decomposed as $W = B + D$. The quantity D describes the energy cost for the de-relaxation, i.e. for the shift of the slab atoms from their equilibrium geometry. This distortion energy can be calculated explicitly and may be interpreted as a destabilizing factor. In order to make the adsorption take place, the total energy W must be negative. This requires that the energy gain $B \leqslant 0$ due to the additionally formed H–Mo bonds is large enough to compensate for the slab distortion and so plays the role of a stabilizing factor.

Table 2. Adsorption of a single hydrogen atom in the unit cell of a nine-layer slab of Mo(111) calculated by DFT. For various adsorption sites, the relaxations of interlayer spacings $\Delta d_{ik}/d_0$, the H–Mo bond lengths, the hydrogen height d_H relative to the top layer, the adsorption energies ΔW (using the H/Mo_3 configuration as a reference) and the distortion energy D of the slab relative to the energy of the clean slab in its equilibrium geometry are given.

	Onefold			Twofold	Threefold
	Mo_3	Mo_2	Mo_1	Mo_1–Mo_2	Mo_1–Mo_2–Mo_3
Δd_{12} (%d_0)	−19	−16	−15	−23	−18
Δd_{23} (%d_0)	−20	−11	−3	−7	−18
Δd_{34} (%d_0)	+ 7	−1	+ 4	+ 1	+ 9
Δd_{45} (%d_0)	+ 6	+ 8	−5	+ 5	+ 3
H–Mo_1 (Å)	2.61	2.79	1.76	1.94	2.10
H–Mo_2 (Å)	2.82	1.82	3.63	1.88	1.91
H–Mo_3 (Å)	1.84	3.69	4.30	3.16	2.08
d_H (Å)	0.37	1.05	1.76	0.92	0.30
ΔW (eV)	Reference	−0.50	+ 0.66	−1.16	−0.87
D (eV)	0.04	0.12	0.35	0.12	0.07

In order to determine the adsorption site of a single hydrogen atom and the de-relaxation that it induces, we optimized several structures where hydrogen is adsorbed at onefold-, twofold- and threefold-coordinated sites. For onefold sites, which are the top sites above atom Mo_1 or Mo_2 or Mo_3 (see figure 1), we used the C_{3v} symmetry as a constraint. Therefore, atoms were allowed to move only along the z-axis, i.e. vertically with respect to the surface. For twofold and threefold sites, geometry optimizations were performed without any constraint, i.e. all atoms were free to displace in all directions until the energy minimum was found. Table 2 provides the corresponding interlayer relaxations, bond lengths and adsorption heights d_H above the top layer. Also, the quantity D and the adsorption energy are displayed, where the latter is expressed by ΔW, i.e. relative to the adsorption energy with H adsorbed on top of Mo_3 used as a reference. The optimized geometries for top sites show that the hydrogen interaction is dominantly with the metal atom above which it resides, corresponding to H–Mo bond lengths of 1.76 Å–1.84 Å. The other H–Mo distances are much larger, 2.60 Å–2.82 Å, and are of rather ionic character, corresponding to electrostatic interactions between hydride H^- and metal cations Mo^+. The bridge site involves both Mo_1 and Mo_2 atoms, with a slightly stronger interaction with the second-layer atom, as is apparent from the respective bond-length values, H–Mo_2 = 1.88 Å and H–Mo_1 = 1.94 Å. The optimization does not lead to bridge sites involving combinations of Mo_1–Mo_3 or Mo_2–Mo_3 atoms. The threefold site simultaneously

involves Mo_1, Mo_2 and Mo_3 atoms with bond lengths of 2.10, 1.91 and 2.08 Å, respectively.

Since the H–Mo bond strength is larger than that of Mo–Mo (2.98 eV [1] versus 1.14 eV [41]), the formation of an H–Mo bond induces a weakening of Mo–Mo bonds between the Mo atom bonded to hydrogen and its first Mo neighbours. As a consequence, for H/Mo_1 the layer interacting with hydrogen undergoes an outward relaxation, i.e. the first spacing relaxes from −23% to −15% (see tables 1 and 2). For deeper layers coordinated with hydrogen, the situation is more complex as the weakening of the bonds to Mo neighbours above and below the layer leads to inward and outward relaxations, respectively. For H/Mo_2 this adds up to an outward relaxation of the second layer (from −21% to −11%), whilst for H/Mo_3 the total relaxation of the third layer is inward (from +12% to +7%). For H at the bridge site, the bonding is stronger with Mo_2 than with Mo_1. So, the second spacing relaxes from −21% to −7% whereas the first distance remains unchanged. We discuss in some more detail the case of H/Mo_1, because we expect the first substrate layer to be involved in the bonding to hydrogen in the experimental situation also.

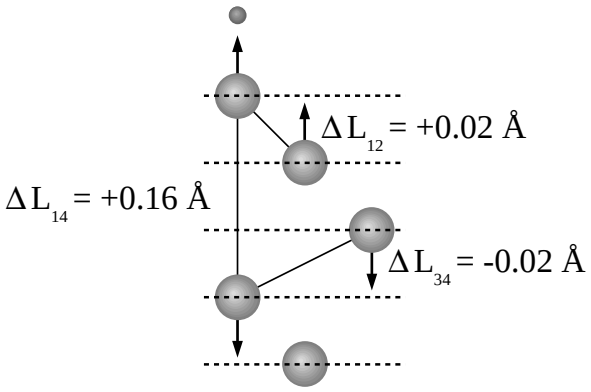

Figure 3. De-relaxation of the second-layer spacing upon adsorption on top of the first-layer molybdenum atoms: the formation of the H–Mo_1 bond leads to a weakening of the Mo_1–Mo_4 bond. Consequently, Mo_4 strengthens its bond with Mo_3, and the third layer shifts inward, which leads to an increase of the interlayer spacing d_{23}.

Although the de-relaxation of the first spacing for H/Mo_1 can be understood as the consequence of a direct effect of hydrogen adsorption, it is not obvious why the second spacing is completely de-relaxed (from −21% to −3%). This de-relaxation is due to the weakening of the interaction of Mo_2 with Mo_3 and Mo_5 atoms according to which the respective bond lengths increase: Mo_2–Mo_3 by 0.04 Å and Mo_2–Mo_5 by 0.03 Å. In fact, the formation of the H–Mo_1 bond leads to the weakening of that of Mo_1–Mo_4; the bond length increases from 2.46 Å for the clean surface to 2.62 Å. Consequently, Mo_4 strengthens its bond with Mo_3 (the bond length decreases by 0.02 Å) to the detriment of Mo_2–Mo_3 (see figure 3). The conclusion is that hydrogen relieves the relaxation of the second layer with which it does not interact directly. The effect of hydrogen adsorption that starts on the top layer propagates through the slab to up to the fourth layer. Each metal atom responds to the adsorption by changing its bonding with surrounding atoms. According to the bond-order-conservation model [42, 43] the strengthening of a particular bond of an atom leads to the weakening of its other bonds and vice versa. Therefore, to get a clear picture of the relaxation, one has to take into account the response of all slab atoms to the formation of the H–Mo bond, and these responses are seen in

the change of the local atomic bonding.

The overall charge transfer is a donation of electrons to hydrogen, which is consistent with the larger electronegativity of the hydrogen atom. An indication of this charge transfer is given by both the increase of the electron density inside the hydrogen muffin-tin sphere and the increase of the surface work function upon hydrogen adsorption. The relative values of the calculated energies as given in table 2 show that the most stable adsorption site is the twofold bridge site where hydrogen makes two bonds with the surface involving the atoms Mo_1 and Mo_2. We also see from the table that the variation of the distortion energy is smaller than that of the adsorption energy. Therefore, the difference in adsorption energies is mainly due to the difference in the strengths of H–Mo bonds. In particular, the twofold site is more stable than the threefold site, mainly because the strengths of the two bonds that hydrogen makes at the twofold site are larger than those of the three bonds made at the threefold site. The adsorption on the first layer, H/Mo_1, involves a large distortion energy of +0.35 eV. Moreover, comparison of the strengths of the bonding with the atoms Mo_1 and Mo_3 estimated as the difference $\delta B = \delta(W - D) = \delta(\Delta W - D)$ tells us that the H–Mo bonding for H/Mo_1 is 0.35 eV weaker than that for H/Mo_3, which makes the site on top of Mo_1 very unfavourable for adsorption.

5. Analyses of the Mo(111)-(1 × 1)–3H phase

The Mo(111)-(1 × 1)–3H phase was analysed independently by LEED and DFT. In the following, we first present the LEED analysis, in spite of the rather large uncertainty that we have to expect for the position of hydrogen atoms. However, because of the weak hydrogen scattering, the adsorbate-induced relaxation of the substrate will be found with high precision, largely independently of the accuracy of the knowledge of the hydrogen positions. As it will turn out, this helps to differentiate between different structures found to be of similar total energy by DFT.

5.1. LEED analysis of Mo(111)-(1 × 1)–3H

For the hydrogen-covered surface, the coordinates of the three hydrogen atoms in the unit cell are additional parameters to be determined compared to the case for the clean surface. Although the width of the experimental database ($\Delta E = 3630$ eV) is considerable and should be sufficient for determining a total of about 15 geometrical parameters, the contribution of hydrogen scattering to integer-order spots (remember that there are no superstructure spots) is in our experience too small for deriving the nine hydrogen coordinates reliably. Therefore, we decided to test five different models in which the adatoms reside at differently coordinated sites, but did not allow for the independent variation of all coordinates. As schematically displayed in figure 4(a), these sites could be onefold coordinated, i.e. the adatoms could reside on top of atoms of the first three substrate layers. On the other hand, the sites could be twofold coordinated, where the coordination could be with atoms $Mo_{1,2}$ (as indicated in figure 4(b)), with atoms $Mo_{1,3}$ or with atoms $Mo_{2,3}$. There is only one type of threefold-coordinated site, as displayed in figure 4(c). For this case, two mirror-symmetric domains exist. Domains with twofold-coordinated sites on different terraces separated by surface steps were considered as well; they were given equal weight in the analysis.

In order to restrict the number of hydrogen coordinates, it was assumed that the H–Mo bond lengths in each model of coordination are the same for all coordinating Mo atoms. This bond length was varied in the analysis, which involved both lateral and vertical movements of the hydrogen atoms. As these movements are correlated, it is sufficient to use just a single

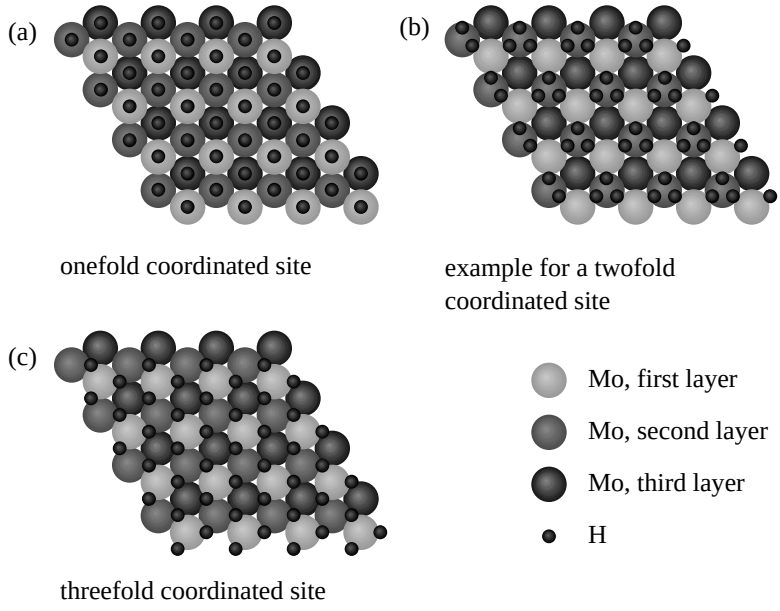

Figure 4. Possible adsorption structures for 3 ML hydrogen on Mo(111) yielding a (1×1) structure: (a) a onefold-coordinated site; (b) an example of a twofold-coordinated site leading to a bridge position between first- and second-layer substrate atoms; (c) a threefold-coordinated site.

parameter for the description of the structure. We choose d_{H}, the vertical distance of the adatoms from the uppermost substrate layer, as is usual in surface structure determination. Of course, the equal-bond-length condition does not need to be met in reality but—as we will see—it still allows us to differentiate to a certain extent between the different models. For the quick test of the models, we used just a restricted data set, i.e. electron energies below 300 eV above which the scattering by hydrogen is negligible anyway. The structure of the substrate used in the TensorLEED reference calculation was obtained by completely neglecting the scattering by hydrogen. This yielded relaxations of the first five interlayer distances of -17.6%, $+1.1\%$, -4.4%, $+4.4\%$, -4.4% which, as it will turn out, are already rather close to the values obtained by the full analysis.

Of the five adsorption models tested preliminarily, the threefold-coordinated hollow-site model yielded the best experiment–theory agreement, according to a Pendry R-factor of $R_{\mathrm{hollow}} = R_{1,2,3} = 0.142$. With the range 50–300 eV used, the variance of the R-factor amounts to $\mathrm{var}(R) = 0.023$. The minimum R-factors obtained for the other four models were $R_{\mathrm{top}} = 0.193$ for the top-site model, and $R_{\mathrm{b1,3}} = 0.189$, $R_{\mathrm{b1,2}} = 0.168$ and $R_{\mathrm{b2,3}} = 0.176$ for the different bridge-site models, where the indices of the R-factor indicate the atomic layer with whose Mo atoms the hydrogen is coordinated. Except for the bridge$_{1,2}$ model, the R-factors for the models are well above $R_{\mathrm{hollow}} + \mathrm{var}(R)$ and so can be discarded. Moreover, the top position and the bridge$_{2,3}$ position led to non-physical hard-sphere radii for the hydrogen atoms ($r_{\mathrm{H}} = 0.41$ Å and $r_{\mathrm{H}} = 0.91$ Å, respectively).

The eventual structural refinement was performed using the full experimental data range, 50–500 eV, in order to provide the highest possible accuracy for the adsorbate-induced substrate relaxation. Although the fit for the bridge$_{1,2}$ model using the reduced data set was only slightly worse than that for the hollow-site model, only the latter model was refined, since

Table 3. The structure of the 3H phase as determined by LEED and DFT. Relaxations of interlayer spacings, H–Mo bond lengths, the H–H distance and the hydrogen adsorption height d_H relative to the top layer are given.

	DFT	LEED
$\Delta d_{12}/d_0$ (%)	−23	-17.4 ± 1.5
$\Delta d_{23}/d_0$ (%)	+ 2	± 0.0
$\Delta d_{34}/d_0$ (%)	−4	−2.2
$\Delta d_{45}/d_0$ (%)	+ 3	+ 4.3
$\Delta d_{56}/d_0$ (%)	—	−3.2
$\Delta d_{67}/d_0$ (%)	—	+ 2.2
H–Mo_1 (Å)	2.01	1.90
H–Mo_2 (Å)	1.82	1.90
H–Mo_3 (Å)	2.41	1.90
H–H (Å)	2.12	1.90
d_H (Å)	0.43	0.03 ± 0.51

the two models do not differ substantially anyway. The best-fit structure of the preliminary analysis was used as the TensorLEED reference. The ten uppermost interlayer distances were varied together with the adsorption height d_H, assuming again that the lengths of the bonds to all coordinating Mo atoms remain the same. The best-fit parameters, relating to a minimum R-factor of $R_{1,2,3} = 0.138$, are summarized in table 3, where the relaxations of very deep layers are again not displayed because they are statistically insignificant. The fit finds the adatoms practically embedded within the top substrate layer ($d_H = 0.03 \pm 0.51$ Å). Although, as argued above and evident from the large error limits for d_H, the LEED determination of the hydrogen position is rather uncertain, the value resulting for d_H is equivalent to a very reasonable hydrogen hard-sphere radius of 0.54 Å. The most surprising result of the analysis, however, is the way in which the substrate interlayer spacings change upon hydrogen adsorption. The pronounced first-layer contraction of the clean surface (−18.8%) remains almost the same, with $\Delta d_{12}/d_0 = -17.4\%$. The second spacing, however, turns out to be completely de-relaxed ($\Delta d_{23}/d_0 = \pm 0.0\%$) and also the following interlayer distances are not very different from the bulk value. The drastic change of d_{23} is also mirrored by the remarkable differences between the spectra of the clean and hydrogen-saturated surface as displayed in figure 2. These differences cannot be caused by mere scattering by hydrogen, in particular not at higher energies. The lower panels of figure 2 also provide a visual impression of the quality of the theory–experiment fit.

5.2. DFT analysis of Mo(111)-(1×1)*–3H*

Although the DFT analysis of the adsorption of a single hydrogen atom per substrate unit cell clearly favoured the bridge site as the adsorption site, we cannot rely on that to hold also when three adatoms are to be accommodated within the cell. Therefore, a new total-energy minimization is necessary. As starting structures we chose different adsorption models using the nine-layer substrate. The adatoms were allowed to move and the substrate multilayer relaxation to modify until an energy minimum was found in each case. The selection of different starting models is used to identify (possibly) different minima of the total energy, the deepest of which will be taken as the likely global minimum corresponding to the true adsorbate structure. Again, both the total adsorption energy ΔW and the distortion energy D of the substrate slab with respect to the layer spacings of the clean surface were calculated. Three starting structures for the (1×1)–3H phase were used. In the first one, the adatoms were

positioned on top of atoms Mo_1, Mo_2 and Mo_3. For this model, the adatoms were allowed to move only vertically. In the two other models, hydrogen atoms were assumed to initially form an equilateral triangle whose centre is positioned on top of one of the two hollow sites, i.e. on top of atom Mo_2 or Mo_3. As the stacking of substrate layers is ABCABC. . ., we use for short the names 3H/'hcp' site and 3H/'fcc' site for the centring on Mo_2 and on Mo_3, respectively. For these starting configurations the adatoms were allowed to move without any constraint.

Except for the on-top sites with the intrinsic single coordination of the adatoms, the energy minimizations landed in geometries with hydrogen atoms twofold coordinated (even when starting, as a test, from a geometry with each hydrogen making three bonds, the optimized geometry leads to twofold coordination). The on-top sites can clearly be ruled out, with ΔW larger by as much as 2.46 eV than the corresponding value for 3H/'fcc' (used as a reference). However, this does not apply for 3H/'hcp', whose total energy is only 0.04 eV larger than that for 3H/'fcc'. In spite of their similar energies, the structures optimized from the 'fcc' and 'hcp' configurations are rather different, in particular as regards the relaxation of the substrate. So, the optimization from the 'hcp' model leads to a strong distortion of the substrate ($\Delta d_{12}/d_0 = -56\%$, $\Delta d_{23}/d_0 = +29\%$) costing a lot of energy ($D = 1.43$ eV), compensated by a strong H–Mo bonding. This result is very unlike that from the LEED analysis and so can certainly be ruled out. The same holds for the hydrogen adsorption height ($d_H = 1.02$ Å). In contrast, the structure optimized from the 'fcc' model fits rather well with the LEED result within the limits of error, as given in detail in table 3.

6. Discussion

Considering the clean surface, we should keep in mind that with the creation of a bcc(111) surface the coordination of top-, second- and third-layer atoms is reduced from 8 to 4, 7 and 7, respectively. The top- (second-) layer atom even has one of its nearest neighbours in the fourth (fifth) layer. The sets of structural results obtained from LEED and DFT both show that an inward relaxation takes place whereby these atoms move directly toward each other in order to partially compensate for the missing bonds. If one compares the absolute bond lengths obtained from LEED and DFT, one must remember that the lattice parameter resulting from DFT is about 1% too large, i.e. the bond length within the volume is 2.75 Å rather than the real value of 2.72 Å which enters the LEED data. In the following, we give the results obtained from LEED and those produced by DFT in brackets. So, atom Mo_1 from the first layer moves inward such that the Mo_1–Mo_2 and Mo_1–Mo_4 bond lengths decrease from the bulk value to 2.66(2.68) Å and 2.43(2.46) Å, respectively. Similarly, atom Mo_2 of the second layer moves inward; the Mo_2–Mo_3 and Mo_2–Mo_5 bond lengths become 2.66(2.70) Å and 2.63(2.67) Å, respectively. Although the magnitude of the relaxation is the same for the first and second interlayer distances, the changes in local bonding are different for the two layers: atom Mo_1 of coordination 4 in the unrelaxed slab strengthens its bonds much more than atom Mo_2 of coordination 7. Evidently, the results obtained from LEED and DFT agree very well; the bond lengths differ by not more than 0.02 Å if one corrects for the $\simeq$1% systematic overestimation by DFT. Agreement is also seen with recent pseudopotential plane-wave calculations, yielding values of -19% and -20% for the relaxations of the first two layer spacings [7]. The different layer relaxation obtained by LEIS [8] might be due to residual gas adsorption, which is practically inevitable in a time-consuming measurement. This suspicion arises from the fact that the LEIS values are very close to those determined in the present analysis for the hydrogen-covered surface and that in many cases the residual gas consists mainly of hydrogen.

Whilst LEED and DFT could be used alone to determine the clean surface structure in

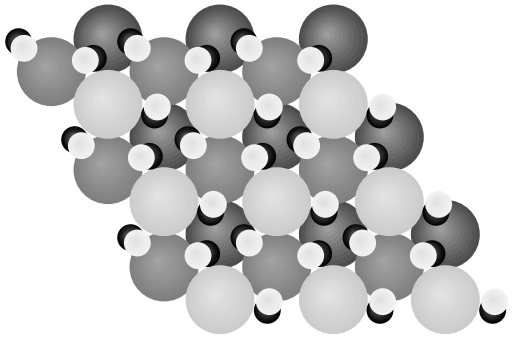

Figure 5. Comparison of the hydrogen adsorption sites obtained from LEED (small dark spheres) and by using DFT (small white spheres).

each case, with excellent agreement with the results, the structure determination of the full adsorption structure of the hydrogen-saturated surface came only from the interplay of the two methods. DFT could not decide between two rather different adsorption structures with very different substrate relaxations involved but exhibiting almost the same total energy. This might suggest that domains with different structures could be present at the surface, at least near zero temperature, for which the calculations were carried out. We cannot exclude this possibility, but we can rule it out through the LEED analysis for liquid-air temperature to which the experiments apply. The strength and accuracy of LEED in determining substrate interlayer spacings clearly favours one of the model structures. The presence of different domains with different sets of layer spacings is most unlikely in view of the low R-factor achieved and in view of the fact that the intensity spectra are fully modulated, i.e. they take zero values at certain energies. This clearly speaks against intensity contributions from differently structured domains. Furthermore, the substrate structure of the thus-favoured model is very close to that determined from LEED. On the other hand, LEED was unable to reliably resolve the exact positions of three hydrogen adatoms in the unit cell due to their weak scattering. As a compromise, only sites of special coordination were tested, where the hydrogen bond lengths within each model were assumed to be equal for all three atoms. As a consequence of this crude approximation, no reliable differentiation could be made between atoms in twofold and threefold coordination, although the best fit corresponds to the threefold-coordinated sites. Here, DFT played its part by clearly favouring the twofold coordination with no local symmetry of the adsorption site. We should emphasize, however, that the best-fit and lowest-energy structures obtained from LEED and DFT, respectively, are not too different, as is obvious from figure 5 which compares the respective hydrogen locations, as differently shaded adatoms, in a top view of the surface. One might imagine that the fit by means of LEED could be improved by using the hydrogen adsorption site obtained by DFT, combined with the substrate multilayer relaxation determined from LEED. However, the corresponding R-factor for the comparison to experimental data turns out to be slightly worse than that for the best-fit model, but is still within the R-factor's variance. The slight increase in the R-factor is probably due to the fact that the substrate relaxation was once again not optimized for the assumed hydrogen position.

It is obvious from the DFT calculations that even with three hydrogen atoms in the surface unit cell a twofold-coordinated site remains the most favoured site, which is occupied when only a single atom per unit cell is adsorbed. Of course, the exact hydrogen positions and bond lengths modify slightly because of slight changes induced by the increased coverage in the

substrate structure. However, no differently coordinated sites are occupied simultaneously as observed in the case of H/Re(10$\bar{1}$0) and H/Ru(10$\bar{1}$0) [4]. Surprisingly, the hydrogen adsorption has practically no influence on the substrate's first-layer spacing, which is fairly independent of the coverage, i.e. its drastic contraction remains quantitatively almost constant. Only layer spacings below are affected—the latter, however, are considerably affected, in particular d_{23}. Its value obviously depends on the amount of hydrogen adsorbed, as becomes clear from the DFT calculations which predict Δd_{23} to relax from -21% of the clean surface (see table 1) to -7% for a hydrogen coverage of 1 (see table 2) and to +2% for hydrogen coverage 3 (see table 3). Apparently, the bonding of hydrogen atoms to atoms Mo_1 and Mo_2 in each case weakens dominantly the Mo_2–Mo_3 and Mo_1–Mo_4 bonding, respectively. This is corroborated by the respective bond lengths: whilst the bond length for Mo_1–Mo_2 remains constant (2.68 Å), that for Mo_1–Mo_4 expands from 2.46 to 2.52 Å, that for Mo_2–Mo_3 from 2.70 to 2.75 Å and that for Mo_2–Mo_5 from 2.67 to 2.76 Å. Yet, in spite of the considerable modifications of substrate relaxations induced by hydrogen adsorption, the corresponding distortion energies are rather small, i.e. the energetics of the adsorbate system is dominated by the bonding of the adatoms to the substrate.

In conclusion, we have shown that surface structure determinations by means of LEED and DFT produce very close results. This is in spite of the fact that the DFT calculations were performed for zero temperature with neglect of zero-point vibrations. One method compensates for the uncertainty of the other when present, so a complete model of the adsorbate structure including the adatom positions and the substrate relaxation can be derived. For the special surface under consideration, a drastic double contraction of layer spacings at the surface of clean Mo(111) was found and confirmed to be typical for bcc(111) surfaces. For the hydrogen-saturated Mo(111)-(1 $\times$ 1)–3H phase, twofold-coordinated adsorption sites were identified (slightly shifted away from the ideal bridge site), i.e. not the sites of highest possible (threefold) coordination. This seems to be in some contrast to the cases of other surfaces offering threefold-coordinated sites, but it might be due to the complex geometry/roughness of bcc(111) surfaces and so is not really surprising. However, the substrate relaxation induced by the hydrogen atoms is exceptional and unparalleled in both type and magnitude. Only spacings below the second layer are induced to relax; the drastic contraction of the second spacing de-relaxes completely. The considerable contraction of the uppermost spacing is practically unaffected by adsorption.

Acknowledgments

Financial support was granted by the Deutsche Forschungsgemeinschaft (DFG). MA is grateful for a grant from the 'Studienstiftung des deutschen Volkes'. The authors also greatly appreciate the advice and help of Professor M Scheffler (FHI, Berlin).

References

[1] Christmann K 1988 *Surf. Sci. Rep.* **9** 1
[2] Christmann K 1989 *Mol. Phys.* **66** 1
[3] *Surface Structure Database 2.0* 1995 (Gaithersburg, MD: National Institute of Standards and Technology)
[4] Döll R, Hammer L, Heinz K, Bedürftig K, Muschiol Z, Christmann K, Bludau H, Seitsonen A P and Over H 1998 *J. Chem. Phys.* **108** 8671
[5] Luo J S and Legrand B 1988 *Phys. Rev.* B **38** 1728
[6] Holzwarth N A W, Chervenak J A, Kimmer C J, Zeng Y, Xu W and Adams J 1993 *Phys. Rev.* B **48** 12 136
[7] Che J G, Chan C T, Jian W-E and Leung T C 1998 *Phys. Rev.* B **57** 1875
[8] Overbury S H 1986 *Surf. Sci.* **175** 123

[9] Sokolov J, Jona F and Marcus P M 1986 *Phys. Rev.* B **33** 1397
[10] Yalisove S M and Graham W R 1988 *J. Vac. Sci. Technol.* A **6** 588
[11] Arnold M, Sologub S, Hupfauer G, Bayer P, Frie W, Hammer L and Heinz K 1997 *Surf. Rev. Lett.* **4** 1291
[12] Arnold M, Hupfauer G, Bayer P, Hammer L, Heinz K, Kohler B and Scheffler M 1997 *Surf. Sci.* **382** 288
[13] Estrup P J 1979 *J. Vac. Sci. Technol.* **16** 635
[14] Passler W A, Lee B W and Ignatiev A 1985 *Surf. Sci.* **150** 263
[15] Zaera F, Kollin E B and Gland J L 1986 *Surf. Sci.* **166** L149
[16] Heinz K and Hammer L 1996 *Z. Phys. Chem.* **197** 173
[17] Okada M and Zehner D M, unpublished
[18] van der Veen J F, Himpsel F J and Eastman D E 1982 *Phys. Rev.* B **25** 7388
[19] Heinz K 1988 *Prog. Surf. Sci.* **27** 239
[20] Heinz K 1995 *Rep. Prog. Phys.* **58** 637
[21] Wedler H and Heinz K 1995 *Vacuum* **7** 107
[22] Pendry J B 1974 *Low Energy Electron Diffraction* (New York: Academic)
[23] Van Hove M A and Tong S Y 1979 *Surface Crystallography by LEED* (Berlin: Springer)
[24] Shih H D, Jona F, Jepsen D W and Marcus P M 1981 *Surf. Sci.* **104** 39
[25] Noonan J R and Davis H L 1987 *Phys. Rev. Lett.* **59** 1714
[26] Rous P J, Pendry J B, Saldin D K, Heinz K, Müller K and Bickel N 1986 *Phys. Rev. Lett.* **57** 2951
[27] Rous P J and Pendry J B 1986 *Surf. Sci.* **219** 355
Rous P J and Pendry J B 1986 *Surf. Sci.* **219** 373
[28] Rous P J 1992 *Prog. Surf. Sci.* **39** 3
[29] Kottcke M and Heinz K 1997 *Surf. Sci.* **376** 352
[30] Arnold M, Sologub S, Frie W, Hammer L and Heinz K 1997 *J. Phys.: Condens. Matter* **9** 6481
[31] *American Institute of Physics Handbook* 1972 3rd edn (New York: American Institute of Physics)
[32] Hammer L, Landskron H, Nichtl-Pecher W, Fricke A, Heinz K and Müller K 1993 *Phys. Rev.* B **47** 15 969
[33] Pendry J B 1980 *J. Phys. C: Solid State Phys.* **13** 937
[34] Perdew J P, Chevary J A, Vosko S H, Jackson K A, Pederson M R, Singh D J and Fiolhais C 1992 *Phys. Rev.* B **46** 6671
[35] Blaha P, Schwarz K, Sorantin P and Trickey S B 1990 *Comput. Phys. Commun.* **59** 399
[36] Blaha P, Schwarz K and Augustyn R 1993 *WIEN93* (Vienna: Technische Universität Wien)
[37] Kohler B, Wilke S, Scheffler M, Kouba R and Ambrosch-Draxl C 1996 *Comput. Phys. Commun.* **94** 31
[38] Paul J F and Sautet P 1996 *Phys. Rev.* B **53** 8015
[39] Philipsen P H T, te Velde G and Baerends E J 1994 *Chem. Phys. Lett.* **226** 583
[40] Wiesenekker G, Kroes G J, Baerends E J and Mowrey R C 1995 *J. Chem. Phys.* **102** 3873
[41] *CRC Handbook of Chemistry and Physics* 1996 ed D R Lide and H P R Frederikse (Boca Raton, FL: Chemical Rubber Company Press)
[42] Pauling L 1960 *The Nature of the Chemical Bond* 3rd edn (Ithaca, NY: Cornell University Press)
[43] Feibelman P J 1996 *Surf. Sci.* **360** 297